Interaction Potentials from the Velocity Dependence of Total Atom-Atom Scattering Cross Sections*

ERHARD W. ROTHE, P. K. ROL,† AND RICHARD B. BERNSTEIN‡
Space Science Laboratory, General Dynamics/Astronautics, San Diego, California
(Received 14 February 1963)

Methods are described which yield the interatomic potential energy parameters from the velocity (v) dependence of the total scattering cross section (Q). These are applied to previously reported measurements of the scattering of lithium by the rare gases. The Lennard-Jones (12,6) potential is assumed. The cross sections for scattering by argon, krypton, and xenon had been measured in a "low-energy" region, where $Q(v)$ is undulatory. From the extrema velocities the product $\epsilon\sigma$ may be obtained, where ϵ is the depth of the interatomic potential well and σ is the interatomic separation at the zero of potential energy. From the absolute value of Q, the parameter σ (and thus ϵ) may be determined separately. These quantities were also deduced (although less accurately) for the scattering by helium and neon, which were studied in the "high-energy" region. Using the "experimental" ϵ and σ, theoretical curves of $Q(v)$, calculated by a partial-wave analysis, agree well with the experimental results. A minimum to the number of diatom bound states was also established.

INTRODUCTION

MANY measurements of the total cross section, Q, for atom-atom scattering at thermal energies have been reported. These experiments were often interpreted using the theory of Massey and Mohr (MM),[1] assuming that the attractive portion of the interatomic potential [i.e., $V=-C^{(s)}/r^s$] would usually be dominant in determining the magnitude of Q. MM predicted a monotonic decrease in Q with increasing relative velocity, v. Application of the formula MM to experimental measurements of $Q(v)$ yields s and $C^{(s)}$.

Recent theoretical calculations[2–4] showed that deviations from MM behavior [$\equiv Q_{\mathrm{MM}}(v)$] should occur. In a "low-energy" region these calculations predicted undulatory deviations from $Q_{\mathrm{MM}}(v)$. In a "high-energy" region a monotonic decrease of $Q(v)$ is expected; but the v dependence is determined largely by the repulsive portion of the potential.[3,5] This predicted behavior has been found experimentally.[4,6]

Measurements of $Q(v)$ in the "low-energy" region provide direct information on the product $\epsilon\sigma$, where ϵ is the depth of the interatomic potential well and σ is the interatomic separation at the zero of the potential. The separate parameters ϵ and σ may also be found. In addition, it is possible to establish a minimum to the number of diatom bound states for the system. In the high-energy region, accurate experiments should yield the form of the repulsive potential, as well as the parameters ϵ and σ.[5]

* Supported by Advanced Research Projects Agency (Project Defender) through the U. S. Office of Naval Research.
† On leave from Laboratory for Mass-Separation, Amsterdam, The Netherlands.
‡ GD/A consultant. Address: Chemistry Department, University of Michigan, Ann Arbor, Michigan.
[1] H. S. W. Massey and C. B. O. Mohr, Proc. Roy. Soc. (London) **A144**, 188 (1934).
[2] R. B. Bernstein, J. Chem. Phys. **34**, 361 (1961).
[3] R. B. Bernstein, J. Chem. Phys. **37**, 1880 (1962).
[4] E. W. Rothe, P. K. Rol, S. M. Trujillo, and R. H. Neynaber, Phys. Rev. **128**, 659 (1962).
[5] R. B. Bernstein, J. Chem. Phys. **38**, 515 (1963).
[6] P. K. Rol and E. W. Rothe, Phys. Rev. Letters **9**, 494 (1962).

SEMICLASSICAL PHASE-SHIFT ANALYSIS

In the present analysis, the Lennard-Jones (12,6) potential has been assumed. A semiclassical (SC) approximation was used to compute phase shifts (η_l) and Q's. The method has been previously described.[4]

Checks were made of the accuracy of the SC computer program, as follows. Some "exact" phase shifts were obtained by a numerical (RKG) integration of the radial wave equation. The RKG program (described previously)[7] appears to have a numerical precision of ± 0.01 rad. Table I shows a comparison of phase shifts

TABLE I. A comparison of phase shifts from the RKG integration of the radial wave equation with those from the semiclassical method.

B	A	l	η(RKG)	η(SC)
125.0	15.000	0	−12.05	−12.06
125.0	20.000	9	− 5.28	− 5.29
125.0	20.000	40	0.22	0.22
125.0	30.000	50	0.37	0.37
213.6	27.341	32	3.29	3.30
213.6	42.608	47	2.25	2.24
380.4	30.838	36	5.09	5.06
380.4	47.774	52	3.50	3.52
380.4	72.977	80	2.40	2.39
561.8	45.900	54	5.20	5.17
561.8	71.106	78	3.59	3.57

obtained by the two methods. Values of η_l are tabulated for several values of the parameters $A(\equiv\mu v\sigma/\hbar)$, $B(\equiv 2\mu\epsilon\sigma^2/\hbar^2)$, and l, where μ is the reduced mass and l is the angular momentum quantum number. For the present application, the SC program is about 10^3 faster than the RKG program. For example, a SC calculation of 250 phase shifts listed in Table III of reference 7 (those for $A\geq 15$) required about 10 sec of IBM 7090 computer time.

Some SC total cross sections were compared with Q's

[7] R. B. Bernstein, J. Chem. Phys. **33**, 795 (1960).

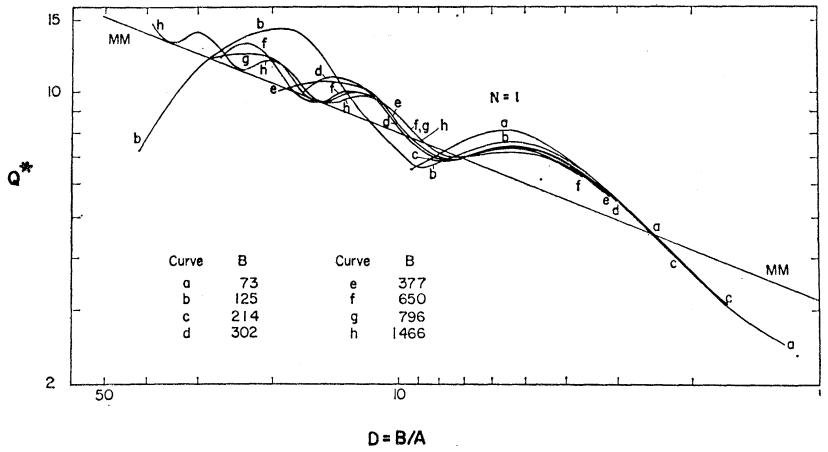

FIG. 1. $Q(v)$, plotted in reduced variables, at several values of B.

previously computed[2] using the RKG program. Q was calculated at $B=125$, for $A=14.1$, 15, 18, 20, 24, and 30. Values within $\pm 1\%$ of those of Table I of reference 2 (RKG calculation) were obtained.

LOW-ENERGY REGION

In this section it will be seen that the product $\epsilon\sigma$ can be obtained to the same accuracy with which "extrema velocities" can be measured. Using this resulting "measured" $\epsilon\sigma$, σ (and thus ϵ) may be obtained independently from the absolute value of Q.

The undulatory (low-energy) region is limited; i.e., approaching from high to low v there is a definite "first" maximum of $Q(v)$. The nomenclature has been previously introduced.[3] The first maximum deviation of Q from Q_{MM} is indexed $N=1$, the first negative extremum is labeled $N=1.5$, etc. The locations of these extrema deviations are not quite the same as those of the absolute extrema of $Q(v)$. Nevertheless, we use the same index notations for both and clarify the type by context.

Figure 1 shows a log-log plot of $Q(v)$ for various values of the parameter B. Plotted are the logarithms of the reduced variables $Q^*\equiv Q/\pi\sigma^2$ and $D^{-1}\equiv A/B=\hbar v/2\epsilon\sigma$. These curves were obtained from the SC analysis except for $B=125$ which was taken from reference 2. Absolute maximum $N=1$ occurs at the same D in all curves, and extrema locations are similar at $N=1.5$, and 2, indicating that $\epsilon\sigma$ is indeed the principal correlating variable, with B the secondary variable.

It is noted that there is a consistent bias of $\langle Q(v)\rangle$ from $Q_{\mathrm{MM}}(v)$, of $7.5\pm 1.5\%$. One might expect[3] $Q_{\mathrm{MM}}(v)$ to pass through the mean of the undulations. This bias is discussed elsewhere.[8]

The locations of the extrema deviations are expressed by

$$N-\frac{3}{8}=0.3012\frac{\epsilon\sigma}{\hbar v_N}\left[1-\frac{0.354(\epsilon/\mu)^{1/2}}{v_N}\right], \qquad (1)$$

where v_N is the velocity of the Nth extremum of deviation. It is shown elsewhere[9] that the $(N-\frac{3}{8})$ replaces the $(N-\frac{1}{4})$ previously used.[3] This relation identifies indices of observed extrema and also yields a numerical estimate of $\epsilon\sigma$. The following procedure may be used: The experimental data are plotted as log Q vs log v, a line of slope $-\frac{2}{5}$ (the MM line) is drawn through the data and the extrema velocities, v_N, are located. Then a plot is made of N vs v_N^{-1}. Arbitrary N's may be used, but the absolute values become obvious from the intercept $(\frac{3}{8})$. Some data treated in this way are shown in Fig. 2, as are the values of $\epsilon\sigma$ which are derived from the limiting slopes.

Because of the curvature, it is difficult to ascertain a precise value for the limiting slope. Nevertheless, the plot yields a good approximation to $\epsilon\sigma$ (i.e., to within $\pm 10\%$) and it identifies the indices. The indexing problem is not always trivial. For example, in a previous paper,[4] $Q(v)$ was computed by the SC method, and was compared to the experimental Li^7-Xe result. Theoretical and experimental maxima happened to coincide near

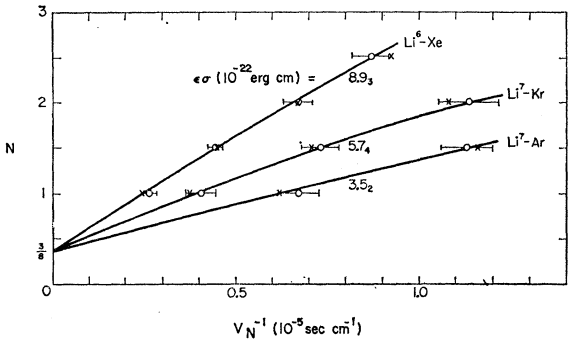

FIG. 2. N vs v_N^{-1} from experimental data. The brackets indicate the uncertainty in locating the extrema. The values of $\epsilon\sigma$ shown are those obtained from the limiting slopes as $v_N^{-1}\to 0$. The crosses show the values predicted from Eq. (1) using the parameters obtained from Table II [i.e., 9.47, 6.09, and 3.82 (10^{-22} erg cm) for Li^6-Xe, Li^7-Kr, and Li^7-Ar, respectively.]

[8] R. B. Bernstein and K. H. Kramer, J. Chem. Phys. (to be published).

[9] R. B. Bernstein, J. Chem. Phys. (to be published).

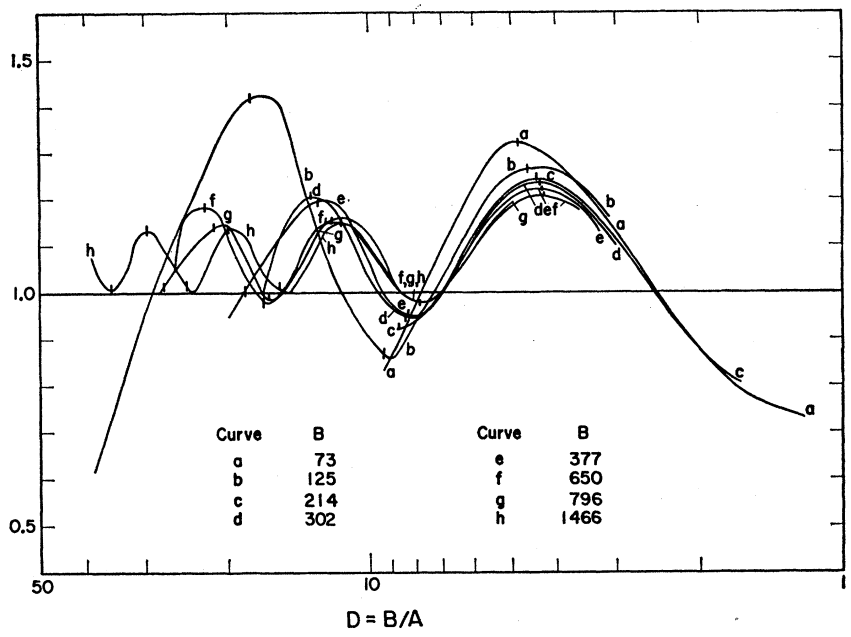

FIG. 3. Q^*/Q^*_{MM} vs D. These coordinates show the extrema deviations as absolute extrema. Tick marks show the extrema locations predicted by Eq. (1).

3500 m/sec. The indexing method later identified the maximum in the theoretical curve as $N=2$, while that in the experimental curve was $N=1$.

To demonstrate the applicability of Eq. (1), extrema deviations were plotted from the computed Q's shown in Fig. 1. The results are drawn in Fig. 3; shown also are tick marks which illustrate the extrema positions predicted by Eq. (1). Agreement is good.

An alternative procedure was employed to obtain the values of $\epsilon\sigma$. This procedure was based on an empirical analysis of the curves of Fig. 1 which indicated that the absolute extrema positions, in the range shown, may be represented by the relation

$$D_N=(m/\mu v\sigma)+a, \tag{2}$$

where $m(10^{-26}$ erg sec$)=0.$, 2.1, 4.5, 7.7, and 14.2; and $a=5.40$, 7.33, 11.9, 13.7, and 18.2 for $N=1$, 1.5, 2, 2.5, and 3, respectively. If the $N=1$ maximum is experimentally obtained, $\epsilon\sigma$ can be found directly. While the determination of $\epsilon\sigma$ from the other extrema requires an assumption of σ, the data are not very sensitive to this assumption.

In Fig. 4 we show two sets of $Q^*(v)$ calculated with the SC program. One of these was obtained with the ϵ and σ finally chosen for the Li^6-Xe system; the other has the same $\epsilon\sigma$, but a different choice of σ. The calculated curve shape is not strongly influenced by the value of σ. However, since the ordinate Q^* is almost the same for both cases, a measurement of the absolute value of Q will yield σ.

These considerations were used in finding the param-

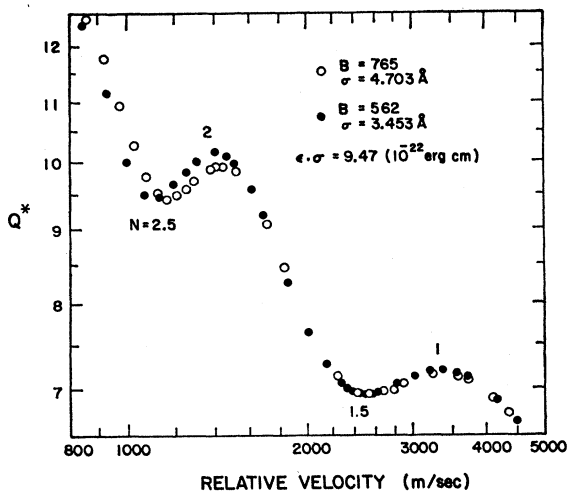

FIG. 4. Two calculated (SC) sets of $Q(v)$. Both sets were computed from the same $\epsilon\sigma$, but a different choice of σ.

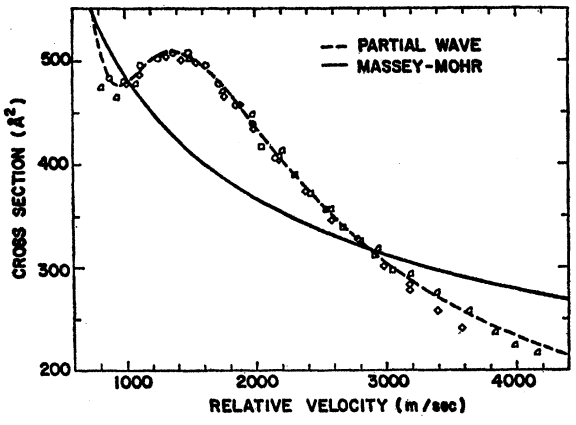

FIG. 5. Scattering of Li^7 by Ar. The theoretical curves were calculated with $\epsilon=8.13\times10^{-15}$ erg and $\sigma=4.70$ Å.

eters for the systems which were studied in the "low-energy" region (i.e., Li-Xe, Li-Kr, and Li-Ar). The extrema are indexed as shown in Fig. 2: The highest velocity maximum observed in each system was $N=1$. After values of $\epsilon\sigma$ were determined from Eq. (2), a trial value of σ was estimated using the MM relation, $Q_{MM}=4.662\times10^{11}(4\epsilon\sigma^6/v)^{2/5}$. Q was computed at one velocity by the SC analysis using this estimated σ. The trial value of σ is then easily corrected, since $Q\propto\sigma^2$. The resulting parameters are listed in Table II. $Q(v)$ was then computed by the SC program. The results are shown in Figs. 5–8.

TABLE II. A summary of the parameters used in the calculations for the curves.

System	$\epsilon\sigma$ (10^{-22} erg cm)	ϵ/k(°K)	σ(Å)	B
Li^7—He[a]	(0.29)	(4.0)	(5.25)	(11.5)
Li^7—Ne	0.80	12.9	4.50	56
Li^7—Ar	3.82	58.9	4.70	320
Li^7—Kr Curve A	6.09	94.0	4.70	554
Li^7—Kr Curve B	6.09	95.7	4.61	543
Li^7—Xe Curve A	9.47	141	4.88	920
Li^7—Xe Curve B	9.47	146	4.70	886
Li^6—Xe[b]	9.47	(146)	(4.70)	(765)

[a] Parameters for helium are less reliable.
[b] Only the product $\epsilon\sigma$ has been experimentally determined for Li^6-Xe.

The values of ϵ and σ in Table II were also used to back calculate v_N using Eq. (1). The results are shown by crosses in Fig. 2. The agreement shows that the method is compatible with Eq. (1).

The Li^7-Ar theoretical curve matches the experimental results within the precision of the experiment, both in the extrema velocities and in the amplitude of undulation.

Two partial wave curves are shown for Li^7-Kr. Curve B better represents the experimental $Q(v)$ at all velocities, while Curve A best fits the (high velocity) $N=1$ maximum. (Since the argon curve was largely fitted to $N=1$, a comparison between the two systems might be better if based upon the fitting the same extremum.) Agreement with experimental data is again good for extrema locations, but the amplitude of the undulation is not well reproduced by the calculation.

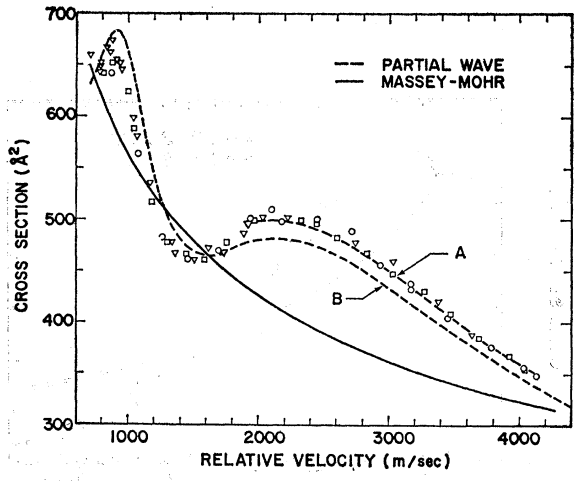

FIG. 6. Scattering of Li^7 by Kr. The partial-wave curve A was calculated with $\epsilon=1.30\times10^{-14}$ erg and $\sigma=4.70$ Å. The partial-wave curve B, and the Massey-Mohr line, were calculated with $\epsilon=1.32\times10^{-14}$ erg and $\sigma=4.61$ Å.

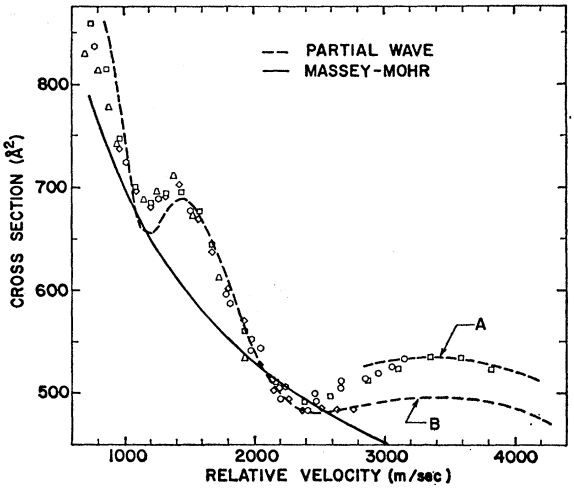

FIG. 7. Scattering of Li^7 by Xe. The partial-wave curve A was calculated with $\epsilon=1.94\times10^{-14}$ erg and $\sigma=4.88$ Å. The partial-wave curve B, and the Massey-Mohr line, were calculated with $\epsilon=2.01\times10^{-14}$ erg and $\sigma=4.70$ Å.

The Li^7-Xe data show the same general behavior as those for Li^7-Kr. Again, the extrema locations are accurate; but the amplitude is not well represented by the calculation. In particular, the $N=1$ amplitude in both cases is larger than the calculated value. The Li^6-Xe data have less scatter; and the $N=1$ maximum is more clearly defined than in the case of the Li^7-Xe. However, the Q's are relative only, and thus the ordinate shown in Fig. 8 refers only to the theoretical values. The theoretical curve is almost identical to that of Li^7-Xe.

Table II shows the final ϵ and σ values used to fit the data. The product $\epsilon\sigma$ was determined within ±2–3%. The separate parameters include an additional uncertainty ($\pm5\%$) which is about half that of the uncertainty of the absolute Q's. Thus, the tabulated ϵ and σ results have a probable error of $\pm6\%$, subject to the constraint of the assumed L-J(12,6) potential.

It might be expected that the mutual consistency of these parameters could be ascertained with the use of known parameters for the rare gases. Unfortunately, the usual "combining laws" are not applicable to systems with widely differing polarizabilities and ionization potentials.[10,11]

Using the experimental values of ϵ and σ (from Table

[10] See, for example, G. Thomaes, R. van Steenwinkel, and W. Stone, Mol. Phys. **5**, 301 (1962).
[11] A. Dalgarno and A. E. Kingston, Proc. Phys. Soc. (London) **73**, 455 (1959).

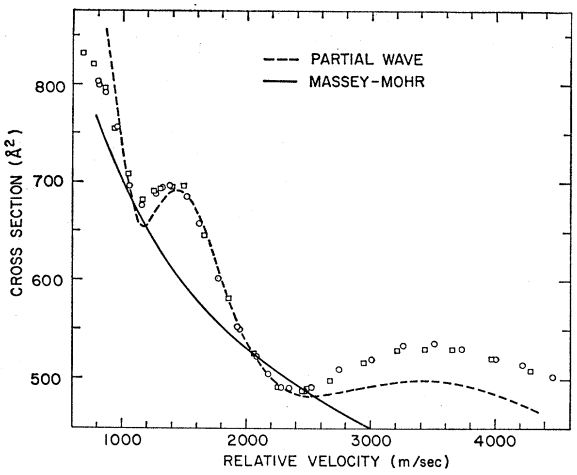

FIG. 8. Scattering of Li^6 by Xe. The theoretical curves were calculated with $\epsilon = 2.01 \times 10^{-14}$ erg and $\sigma = 4.70$ Å. The ordinate is absolute for the calculation but the experimental data were normalized to be equal to that of Li^7-Xe at 2161 m/sec.

II) the long-range inverse sixth-power attractive potential constant, $C^{(6)} = 4\epsilon\sigma^6$, may be calculated and compared with theoretical estimates. Table III summarizes

TABLE III. Comparison of experimental and theoretical C values (10^{-60} erg cm^6).

System Li vs	Experimental	Theoretical[a]	Theoretical[b]
Xe (set *A*)	1052		
Xe (set *B*)	872	459	412
Kr (set *A*)	559		
Kr (set *B*)	509	287	262
Ar	350	191	177
Ne	59	46	46
He	(46)[c]	21	23

[a] See reference 11.
[b] Slater-Kirkwood relation using procedure of E. W. Rothe and R. B. Bernstein, J. Chem. Phys. **31**, 1619 (1959), $\alpha_{Li} = 22$ Å^3, was used [J. C. Zorn and G. E. Chamberlain, Phys. Rev. **129**, 677 (1963); and A. Salop, E. Pollack, and B. Bederson, *ibid.* **124**, 1431 (1961)].
[c] This value is less reliable than others.

the results. As previously noted,[12] the experimental values are about twice those predicted by perturbation theory calculations.

It is also of interest to predict from the ϵ values the locations of the classical "rainbow angle" θ_r in the differential scattering cross sections (not yet studied). Using procedures previously described,[13] and assuming the L-J(12,6) potential, one expects the following rainbow angles (in the c.m. system): Li^7-Ar, 20°; Li^7-Kr (Set *B*), 30°; Li^7-Xe (Set *B*), 46°; and Li^6-Xe, 54° (all for $v = 1000$ m/s). For Ne and He the rainbow angles are expected to be smaller; however, since the ϵ's are less reliable, θ_r values are not listed.

[12] See, for example, E. W. Rothe, L. L. Marino, R. H. Neynaber, P. K. Rol, and S. M. Trujillo, Phys. Rev. **126**, 598 (1962).
[13] F. A. Morse and R. B. Bernstein, J. Chem. Phys. **37**, 2019 (1962).

HIGH-ENERGY REGION

The "high-energy" region has been discussed in two previous papers.[3,5] One of these[3] used the L-J(12,6) potential, while the other[5] treated a general n, 6 potential as well as an exp-6 (α) potential with variable α. The present analysis is confined to the L-J(12,6) potential because the data could, thereby, be sufficiently well fitted.

The appropriate parameters in the high-energy region may be found as follows: A log-log plot is made of the $Q(v)$ data and matched to reduced parameter plots such as Figs. 4 and 5 of reference 5, which show Q^* vs D. By finding corresponding values of D and v the value of $\epsilon\sigma$ is determined. Then, by comparing the experimental values of Q with the Q^* from the reduced plot, the value of σ is obtained.

In order to fit the Li-Ne data, the procedure had to be modified, because the parameters obtained from this procedure showed that D was greater than unity in the lower velocity range (the method is somewhat inaccurate here[3]). The ϵ and σ were, therefore, adjusted empirically until a SC fit was obtained. The results are shown in Fig. 9. All lines shown are drawn using the final chosen value of ϵ and σ. The $s = 12$ line was obtained from the equation[3] for a pure 12th power repulsion, i.e., $Q^* = 2.273 D^{2/11}$. The Q_{JB} line was calculated by the formula given in reference 3. It differs somewhat from the partial-wave calculation. At lower velocities this might be expected because of approximations in the JB formula, but this difference should decrease at higher velocities. The origin of the difference is not clear.

The helium results are shown in Fig. 10. $Q(v)$ is rather flat compared to the other gases, which is characteristic of the "high-energy" region. It was difficult to obtain definitive helium parameters by the "high-energy" procedure, because the uncertainty in the data allows them to be fitted by a range of values. Furthermore, the experimental absolute Q's happen to be less accurate

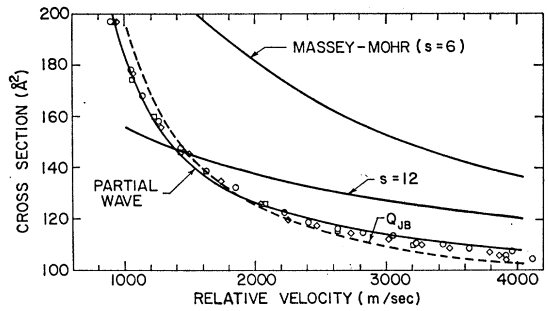

FIG. 9. Scattering of Li^7 by Ne. The theoretical curves were calculated with $\epsilon = 1.78 \times 10^{-15}$ erg and $\sigma = 4.50$ Å.

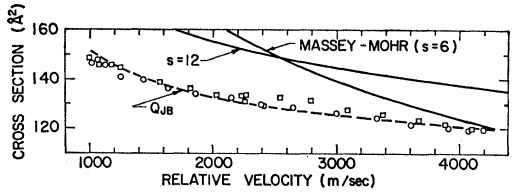

FIG. 10. Scattering of Li^7 by He. The absolute experimental values of Q are less reliable than those for the other gases. The theoretical curves were calculated with $\epsilon=5.5\times10^{-16}$ erg and $\sigma=5.25$ Å.

than those of the other gases.[14] Thus, the ϵ and σ listed in Table II may be in error by $\pm15\%$. Figure 10 shows Q_{JB}, and lines corresponding to the Massey-Mohr dependence ($s=6$) and the pure 12th power repulsion ($s=12$).

DIATOM BOUND STATES

For the Li-Xe systems the lowest velocity extremum is the $N=2.5$ minimum. This strongly suggests the presence of at least one further maximum, $N=3$, and this in turn implies[8,9] a minimum of *three* bound states (vibrational levels of zero angular momentum) for the LiXe ($^2\Sigma^+$) molecule. A similar argument may be applied to the Ar data, yielding a minimum of *two* bound states for LiAr ($^2\Sigma^+$). For LiKr ($^2\Sigma^+$), with $N=2$ observed, the evidence is clear for the existence of a minimum of *two* discrete levels. These experimental results are compatible with the theoretical maximum[15] number (n_0) of bound states for L-J(12,6) wells with the given parameters B (taken from Table II), as listed in Table IV. Additional measurements at lower v for all systems would be of interest, as they should reveal a number of (further) extrema, indicative of the remaining diatom bound states.

TABLE IV. Theoretical maximum number of bound states, n_0, assuming potential parameters of Table II.

Li^7-	Xe	Kr	Ar	Ne	He
B	886	543	320	56	11.5
n_0	8	6	5	2	1

TABLE V. Summary of "best" parameters for lithium–rare gas diatomic molecules in $^2\Sigma^+$ state.

Molecule	$D_e(10^{-3}$ eV)	r_e(Å)
LiXe	12.6	5.28
LiKr	8.24	5.18
LiAr	5.08	5.27
LiNe	1.11	5.05
LiHe[a]	(0.34)	(5.89)

[a] Parameters for helium are less reliable.

In this context it is of interest to convert the potential parameters from Table II into a final summary table for "best" values (from Curves B for Li^7-Xe and Li^7-Kr) using conventional spectroscopic notation [i.e., $D_e(\equiv\epsilon)$ and $r_e(=2^{1/6}\sigma)$] appropriate to diatomic molecules. These are listed in Table V.

[14] Experiments are in progress which should reduce the experimental scatter for Li-He, and determine the absolute value of Q with greater precision.

[15] H. Harrison and R. B. Bernstein, J. Chem. Phys. (to be published).